Gümüşhane University Journal of Science

GUFBD / *GUJS* (2024) 14(4): 980-991 doi: 10.17714/gumusfenbil.1462251 Research Article

Application and comparison of theoretical approaches to mechanical properties of bulk YBCO-358 ceramic superconductors

Yığın YBCO-358 seramiklerinin mekanik özelliklerine teorik yaklaşımların uygulanması ve karşılaştırılması

Fatih BULUT*

Scientific and Technological Research Applications and Research Center, Sinop University, Sinop, Turkey

• Received: 31.03.2024 • Accepted: 19.08.2024

Abstract

Co nanopowder substituted YBCO-358 ($Y_3Ba_5Cu_{8-x}Co_xO_{18-\delta}$) bulk ceramics were prepared with weight ratios of x=0, 0.05, 0.10 and 0.15 using the SSR (Solid State Reaction) method in tube furnace at oxygen (O_2) atmosphere. The impact of partially replacing Cu with Co impurities on the load-independent (or true) microhardness parameters of YBCO-358 have been examined using five theoretical models: Meyer's law (ML), Hays-Kendall (HK), elastic/plastic deformation (EPD), proportional sample resistance (PSR) and the last is indentation-induced cracking (IIC). These models were applied to results that obtained by experimental microhardness tests conducted at various loads. Vicker's Microhardness analysis shown that each samples has reverse indentation size effect (RISE). The results showed that partial Co nanoparticle doping affected the mechanical behavior/properties of produced YBCO-358 ceramics due to an enhance in crystal structural defects. Additionally, the degradation of the crystal structure led to a reduce in the typical RISE behavior of YBCO-358 superconducting ceramics. It has found that the IIC model was the best fit as it was the only one that produced results close to the saturation point, while the other models did not.

Keywords: Microhardness modelling, Solid state reaction method, Vicker's, YBCO

Öz

Co nanotoz katkılı YBCO-358 ($Y_3Ba_5Cu_{8-x}Co_xO_{18-\delta}$) yığın seramikleri katı hal reaksiyon (SSR) yöntemi kullanılarak, tüp fırın içerisinde oksijen (O_2) atmosferinde x=0, 0.05, 0.10 ve 0.15 yüzde ağırlık oranlarıyla hazırlanmıştır. Cu'nun Co safsızlıklarıyla kısmen yer değiştirmesinin YBCO-358'in yükten bağımsız (veya gerçek) mikrosertlik parametreleri üzerindeki etkisi beş teorik model kullanılarak incelenmiştir: Meyer yasası (ML), Hays-Kendall (HK), elastik/plastik deformasyon (EPD), orantısal numune direnci (PSR) ve sonuncusu girinti kaynaklı çatlamadır (IIC). Bu modeller, çeşitli yüklerde yapılan deneysel mikrosertlik testlerinden elde edilen sonuçlara uygulanmıştır. Vicker'in Mikrosertlik analizi, her numunenin ters girinti boyutu etkisine (RISE) sahip olduğunu göstermiştir. Sonuçlar, kısmi Co nanoparçacık katkısının, kristal kusurlardaki artış nedeniyle, üretilen YBCO-358 seramiklerinin mekanik davranışını/özelliklerini etkilediğini göstermiştir. Ek olarak kristal yapının bozulması, YBCO-358 süper iletken seramiklerin tipik RISE davranışında bir azalmaya yol açmıştır. IIC modelinin doyum noktasına yakın sonuçlar üreten tek model olması nedeniyle en iyi uyum sağladığı, diğer modellerin ise uyumsuz olduğu bulmuştur.

Anahtar kelimeler: *Katıhal reaksiyon yöntemi, Mikrosertlik modelleme, Vicker's, YBCO*

*Fatih BULUT; fatihbulut@sinop.edu.tr

1. Introduction

The discovery of high-temperature superconductors (HTSC) has opened new possibilities for practical applications due to its high critical current density (J_c) under high magnetic fields, allowing it to trap magnetic fields and having well pinning properties. Since the time that high-temperature superconductors have discovered, many efforts have been made to improve its superconducting properties such as superconducting transition temperature (T_c), critical current density (J_c), and upper critical magnetic field (Sahoo, Mohapatra, et al., 2019; Yao & Ma, 2021). High Temperature Superconducting (HTS) materials are not single elements, but composite materials that can be formed as a result of mixing more than one element in specific proportions and exposure to special conditions (pressure, high temperature, etc.) (Sahoo, Routray, et al., 2019). Since 1986, researchers have been investigating high-temperature superconductivity in an effort to discover new superconducting materials with a higher Tc. The materials in question, referred to as ceramics, exhibit insulator properties at room temperature due to the minimal interaction between the electrons and the solid lattice structure. Despite being insulators at room temperature, ceramics exhibit a different behavior when cooled below their critical temperature. At this point, the electrons unite and move in harmony with the vibrating lattice, leading to a balance between them. High-temperature superconductors are known for their wide penetration depth, short coherence length, weak charge density, and strong anisotropic properties. These properties make them highly sought after for miscellaneous applications (Sarıtekin et al., 2014).

Superconducting compounds are characterized by their weak flexibility and high brittleness, which negatively impacts their mechanical properties and limits their use in useful applications. To utilize high-temperature superconductors in industrial applications effectively, it is essential to evaluate not only their superconductivity behaviors like critical current, critical magnetic field, density and critical temperature, but also their mechanical characteristics like stiffness, fracture toughness, and hardness. In order to make superconducting materials more practical, researchers have focused on improving their mechanical properties. An effective way to evaluate these properties is through the use of non-destructive techniques like the Vickers microhardness test, which can be easily applied without damaging the material. Hardness is a mechanical property that is closely linked to the structure and composition of the solid, and can be measured using standard materials such as hardened steel, tungsten carbide, or diamond (Kölemen et al., 2006; Saritekin & Üzümcü, 2022). The advancement of the mechanical characteristics of materials that have superconductivity has become a crucial area of study in this field. The mechanical properties of ceramics superconductors such as hardness, elastic modulus and yield strength are vital for their use in industrial applications, such as the manufacturing of superconducting wires (Asikuzun & Ozturk, 2018; Imran et al., 2020; Koralay et al., 2013; Mohammed et al., 2011). Although the replacement of cobalt with copper does not affect the system structurally, it is envisaged that the materials produced in terms of hardness can be adapted to cables and similar technologies.

In this study, the $Y_3Ba_5Cu_{8-x}Co_xO_{18-\delta}$ system (x = 0, 0.05, 0.1, and 0.15) was manufactured via the SSR method, and the mechanical properties of the produced samples were characterized by one of the most common methods which is Vickers microhardness tests. This study explores the effect of substituting a portion of Cu inclusions with Co inclusions in YBCO-358 ceramics on the true microhardness parameters using both experimental and theoretical methods. The research utilizes five theoretical models based on Vickers microhardness tests performed at different applied loads: minimum and maximum loads chosen as 0.245 N and 2.940 N respectively. The analysis of the dopant mechanism and its relationship to material science and engineering principles may provide insights into potential areas of growth and development for the YBCO-358 superconducting matrix.

2. Experimental process

Solid-state reaction has been selected as a production method. Producing samples in right stoichiometries is one of the important parts on superconducting production and so, Y_2O_3 (%99.99 Yttrium (III) oxide), $BaCO_3$ (%99.95 Barium carbonate), CuO (%99.9995 Copper (II) oxide) and Co nanopowder (%99.5 325 mesh-Cobalt powder) powders weighed in calculated amounts. Doping of Co nanopowder is calculated between 0 - 0.15. Obtained mixed powder have been grinded in an agate minimum 1 hour. To prepare the ceramic superconductors, the obtained powders which are mixed and grinded were calcined in the crucible that chosen as alumina to avoid impurities in an air atmosphere at 850°C for 24 hours. To remove residuals process applied three times respectively, with the powders being ground again after each calcination. The powders were pressed carefully via hydraulic press to create bulk samples with 13mm-2mm diameter and thickness

respectively. By pressing the calcined powders, bulk samples obtained. The obtained bulk samples were heated in a tube furnace for 24 hours in an air atmosphere at 930°C. After calcinating, the samples were cooled down to 500°C in a controlled way with a rate of 10 °C/min and sintering process applied in an oxygen atmosphere for 5 hours. After cooling process, the samples were left to reach room temperature. YBCO-358 samples that produced in the study were named 0-Co, 5-Co, 10-Co, and 15-Co according to applied doping amounts (0.00, 0.05, 0.10, and 0.15).

This study determined the mechanical properties of the Co nanoparticle doped and undoped samples by performing Vickers microhardness measurements via Shimadzu HMV-2 tester. The tests were done on the samples at different indentation loads, that range from 0.245 N to 2.940 N. Superconducting properties of the samples have been determined via cryogenic system and four probe method.

3. Results and discussions

The results of the resistance vs time measurements which proofs the superconducting properties of produced samples are given in Figure 1. All samples have superconducting behavior, but the critical temperature values are decreased by increasing of doping ratios. This behavior is expected because of doping element is adding more electron to the system. T_C^{onset} and T_C^{offset} are the critical transition temperature values, at which superconductivity starts to happen and the sample reaches fully superconductivity. Table 1 lists the samples' critical transition temperature values, and superconducting temperature transition width (ΔT_C).

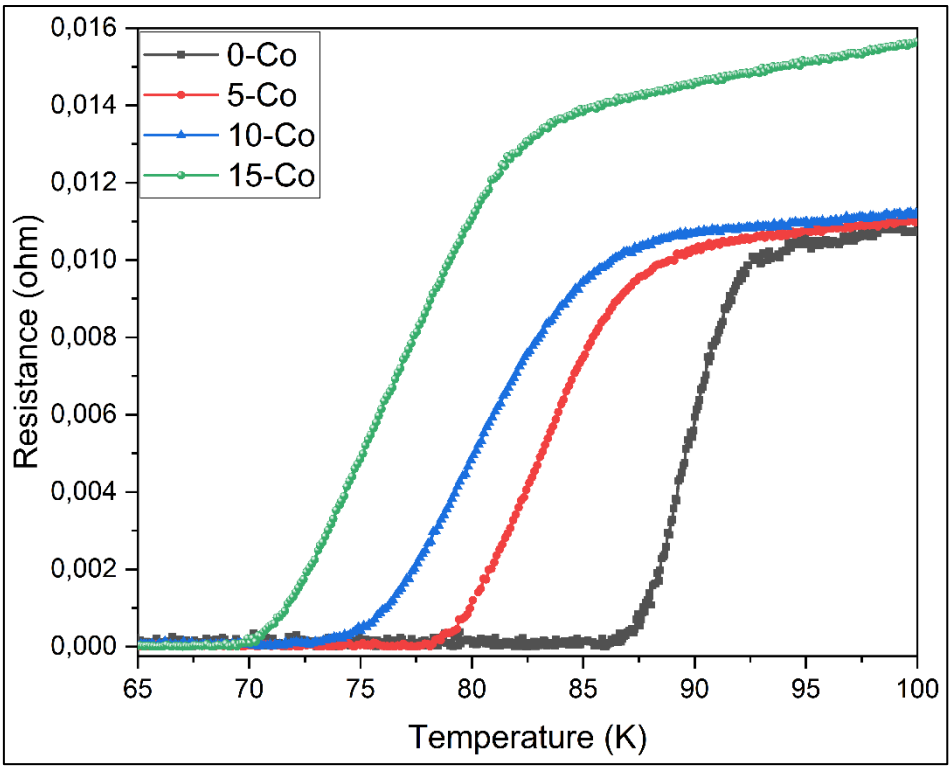

Figure 1. Resistance vs Temperature measurements of produced samples.

Co nanoparticle doped samples subjected to the Vickers microhardness test. The effect of partial substitution of Cu containment with Co impurities on the mechanical behaviors and performance of materials that have YBCO-358 matrix will be examined as a function of substitution level and the indentation test loads (0.245, 0.490, 0.980, 1.960 and 2.940 N, respectively) applied to the Co nanoparticle doped samples. The impact of the Cu-site Co partial substitution on the HV (Vickers microhardness) parameters will be described. The microhardness results of the samples produced will be examined and their characteristic behavior, like Reverse Indentation Size Effect (RISE) or Indentation Size Effect (ISE), will be determined.

Table 1. The critical transition temperature, and superconducting transition width values of the samples.

Samples	T_C^{onset}	T_C^{offset}	ΔT_C
0-Co	92.5	86.2	6.3
5-Co	88.2	78.2	10
10-Co	85.6	72.8	12.8
15-Co	83.5	69.8	13.7

Microhardness test is a method that measures the microhardness and determine the mechanical/micromechanical properties of the samples. It involves measuring the diagonal lengths of an indentation trace which left by a special indenter tip that has pyramidal shape under different loads to determine the Vickers microhardness values. The Vickers microhardness (Hv) parameters at variety of test loads can calculate using the following equation:

$$F = 1854.4 \frac{F}{{d_{ort}}^2} \quad (1)$$

in this equation, Hv is the Vickers microhardness value, the average of the diagonal length is represented by d_{ort}, and F represents the load that applied on the materials surface (Zalaoglu et al., 2020). The HV values of the Co doped and undoped YBCO-358 samples produced is graphically visualized in Figure 2, and it was found that the doping of Co nanopowder to the YBCO-358 matrix rapidly diminishes the mechanical properties and microhardness. The microhardness values of produced samples decrease as the Co nanopowder doping ratio increases, with the greatest reduction occurring at doping ratio of 15%. The change in microhardness values can be clearly seen via Figure 2 and the values from Table 2. For minimum test load (0.245N) while the 0-Co sample has 4.441 GPa, 15-Co sample has 3.445 GPa, but 10-Co sample has the minimum microhardness value (2.119 GPa). As the Co nanoparticle doping ratio increases, the plateau region of the samples was found to decrease. The calculation of the elastic modulus (E) brittleness index (KIC) and yield strength (Y) of the samples have been achieved by the related formulas at ref Asikuzun et al., 2019.

Table 2. H_v, E, K_{IC}, and Y values of the samples produced.

	F (N)	H_V (GPa)	E (GPa)	Y (GPa)	K_{IC} (Pa/$m_{1/2}$) x10^3
	0.245	4.441	363.964	1.48	-457.136
	0.49	5.4	442.618	1.8	-504.116
0-Co	**0.98**	6.8	557.318	2.267	-565.676
	1.96	7.763	636.256	2.588	-604.411
	2.94	7.607	623.477	2.536	-598.31
	0.245	3.33	272.963	1.11	-350.273
	0.49	4.078	334.253	1.359	-387.608
5-Co	**0.98**	5.226	428.322	1.742	-438.773
	1.96	5.64	462.241	1.88	-455.816
	2.94	5.618	460.49	1.873	-454.952
	0.245	2.119	173.654	0.706	-312.144
	0.49	2.94	240.935	0.98	-367.673
10-Co	**0.98**	3.535	289.777	1.178	-403.222
	1.96	4.123	337.899	1.374	-435.417
	2.94	4.304	352.789	1.435	-444.908
	0.245	3.445	282.393	1.148	-336.234
	0.49	4.046	331.597	1.349	-364.351
15-Co	**0.98**	4.695	384.788	1.565	-392.487
	1.96	5.333	437.11	1.778	-418.321
	2.94	5.391	441.832	1.797	-420.575

The study found that as the compression load increased in the range of 0.245 N to 2.940 N, the microhardness values of the samples increased. Upon examination of Figure 2 and Table 2, it was observed that the hardness

values of undoped and Co nanoparticle doped samples enhanced as the load values enhanced. The data suggests that there is a point at which the hardness of the material does not change significantly with further increases in compression load, this point is observed at 2 N. As the Co doping ratio increases, the microhardness values decrease. This decrease is believed to be caused by the presence of impurities, non-uniform crystal structures and the presence of Co atoms between the grains, which may weaken the strong bonds and lead to a reduction in microhardness. All these factors may contribute to an overall decrease in the mechanical properties of the Co nanoparticle doped samples (Asikuzun et al., 2019; Badreddine et al., 2020; Dogruer et al., 2013). The phenomenon of increasing microhardness values with applied load is known as RISE (Dey & Mukhopadhyay, 2014; Sangwal, 2000). This means that smaller indentation loads result in smaller hardness values.

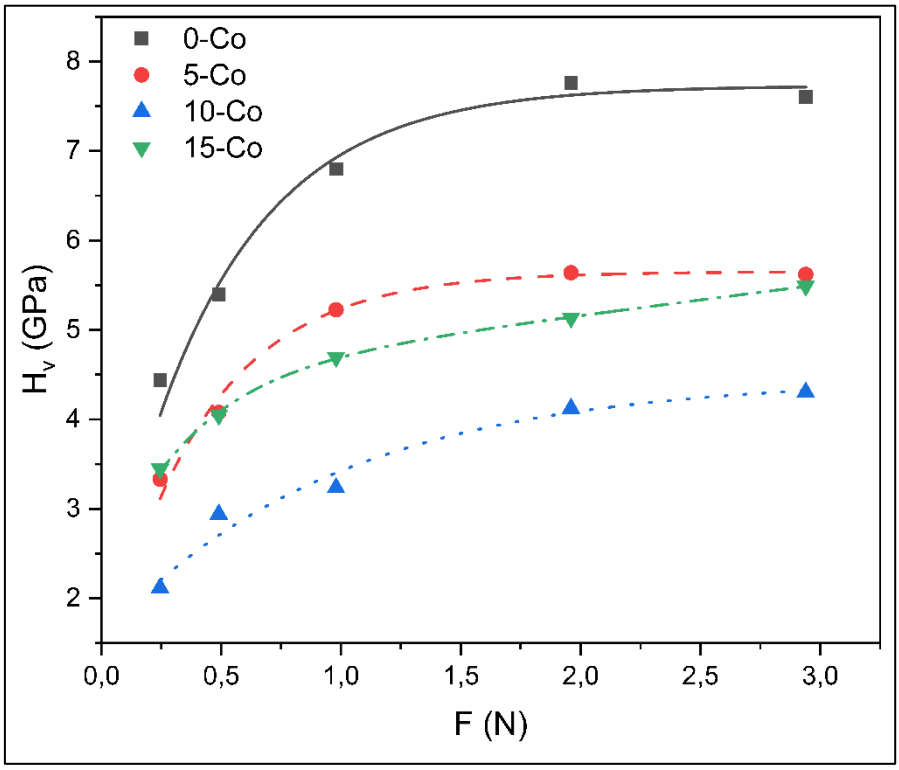

Figure 2. Plot of load dependent Vickers' microhardness (H_V) with applied force F

From Figure 2, produced samples in this study exhibited RISE behavior. It is worth mentioning that the material's behavior remained consistent, however, the microhardness values were found to fluctuate by the increase of Co nanoparticle doping. This study also evaluated other mechanical characterization parameters in addition to microhardness such as load-dependent elastic modulus, yield strength, and fracture toughness (Sedky et al., 2020). Parameters like E, Y and K_{IC}, which are related to microhardness, are considered to be equally important in determining the mechanical properties of many substances. In Table 2, such parameters are calculated and presented, and it was observed that their values were affected by Co nanoparticle doping.

3.1. Meyer's law

The Meyer's law is frequently used by researchers to study the variations in the load-independent mechanical behavior of superconducting ceramic compounds that result from variations in preparation conditions such as partial substitution, addition, doping and annealing processes like pressure, temperature, calcination, sintering ambient atmosphere, and time as well as dopant process. This allows them to understand the impacts of such factors on the micromechanical or mechanical properties of materials (Awad et al., 2011; Rekaby et al., 2022). One of the advantages of the ML (Meyer's law) equation is that it can produce useful, valid, and dependable results for superconducting materials that exhibit both RISE and ISE behaviors. This is due to the strong and sensitive relationship between the exponential power of n and the external test loads, which is linked to the indenter diagonal length. This feature enables the model to accurately capture the microhardness behaviors of the produced materials under varying loading conditions (Anas et al., 2017).

$$F = A_M d^n \quad (2)$$

A_M is the Meyer constant n is the Meyer number, diagonal length of the indentation tip was represented by d. The Meyer's law equation enables the estimation of a material's mechanical behavior based on its Vickers microhardness parameters and the Meyer number, which denotes the applied indentation test load. Materials that exhibit a Meyer number less than 2 show a characteristic indentation size effect, while materials with a Meyer number greater than 2 exhibit the RISE. In the literature it reveals that the value of n is between 1 and 1.6, material classifies as hard; if n>1.6, material classifies as soft (Ozturk et al., 2018). In this study all n values are bigger than 1.6 so all samples produced can be classifies as soft materials.

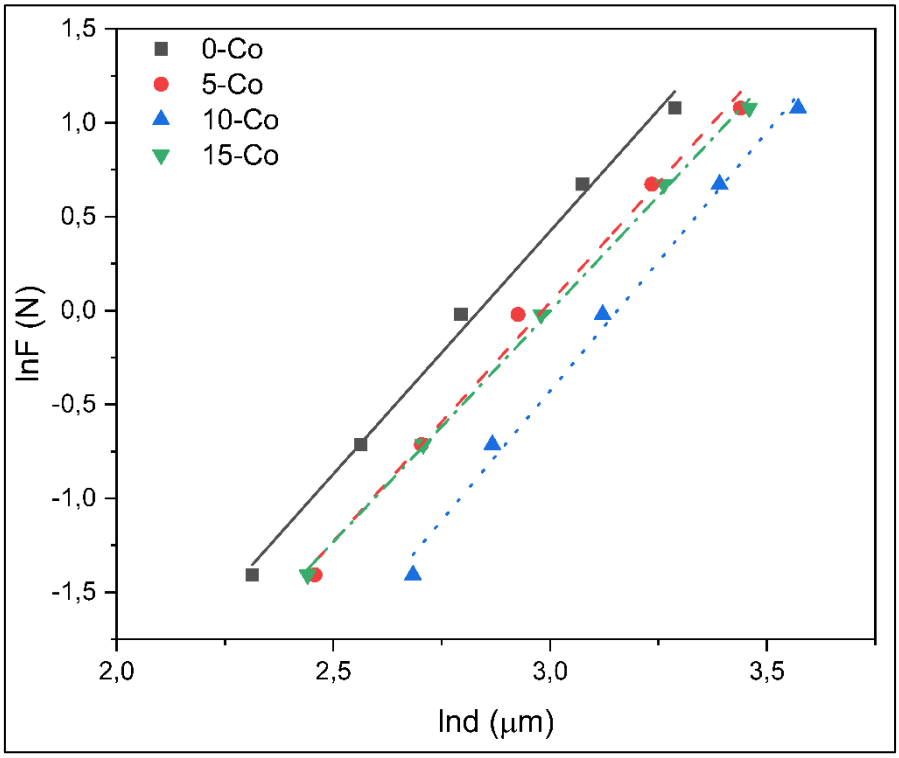

Figure 3. Plots of lnF vs lnd of the samples produced.

According to the ML, slope of the lnF-lnd graph (Figure 3) returns the Meyer number (n value). The analysis of Figure 3 shows that the n values for Co nanoparticle doped samples were greater than 2 (Table 3), indicating a RISE behavior for the materials. The values obtained means that microhardness values increased with the indentation test load that applied.

Table 3. Experimental data according to ML, HK, EPD, PSR and IIC model

	Meyer's Law		**HK**		**EPD**		**PSR**		**IIC**	
Sample	**n**	**A_Mx10^{-3} (N/μm^2)**	**A_{HK}x10^{-2} (N/μm^2)**	**W (N)**	**d_e (μm)**	**A_{EPD}x10^2 (N$^{1/2}$/μm)**	**α (N/μm)**	**β x10^2 (N/μm^2)**	**K $\left(\frac{N^{(3-5mA)/3}}{\mu m^{(2-3m)}}\right)$**	**m**
0-Co	2.586	0.652	0.447	-2.165	-0.248	0.554	-0.029	0.530	310.288	0.457
5-Co	2.547	0.502	0.326	-1.932	-0.226	0.399	-0.022	0.383	269.347	0.452
10-Co	2.757	0.167	0.257	-3.126	-0.332	0.335	-0.028	0.313	322.618	0.482
15-Co	2.456	0.629	0.331	-1.899	-0.202	0.368	-0.020	0.357	202.656	0.421

3.2. Hays and Kendall approach

The Hays and Kendall (HK) approach can be used for examining the load-independent mechanical properties of Co-doped YBCO-358 materials. The approach is particularly useful to examine materials with ISE behavior and involves the concept of a critical indentation test load (W) that causes plastic deformation in the material's crystal structure. The Hays and Kendall approach was utilized to investigate the fundamental mechanical properties of bulk polycrystalline YBCO-358 superconducting ceramic materials in this research. The HK approach offers to a critical indentation test load (W), which is responsible for initiating plastic deformation in a material. So, the effective load was defined in the HK approach F_{eff}=F-W (Erdem et al., 2021; Hays & Kendall, 1973).

$$F - W = A_{HK} d^2 \tag{3}$$

W in the formula is the minimum load and A_{3HK} is the microindentation hardness. The microindentation hardness constant (A_{HK}) and indentation test load (W) are calculated using data extrapolation from measured values of d over applied test load (Table 3). Figure 4 shows the F–d^2 graph which used to obtain values for HK approach. The A_{HK} values obtained as 0.447 N/μm^2 for the 0-Co sample, the A_{HK} reduced with the increasing of Co nanoparticle doping ratio and reached the value of 0.331 N/μm^2 for the 15-Co sample (Table 3). Consistent with the approach, the negative W_{HK} value indicates that the applied load is sufficient to cause plastic deformation, but not enough to produce elastic deformation. Also, negative W_{HK} values indicates the RISE behavior of produced samples (Senol et al., 2019; Soykan et al., 2020). The independent microhardness values that calculated were not consistent with the plateau region, indicating that the Hays and Kendall approach may not be effective to determine the true microhardness values.

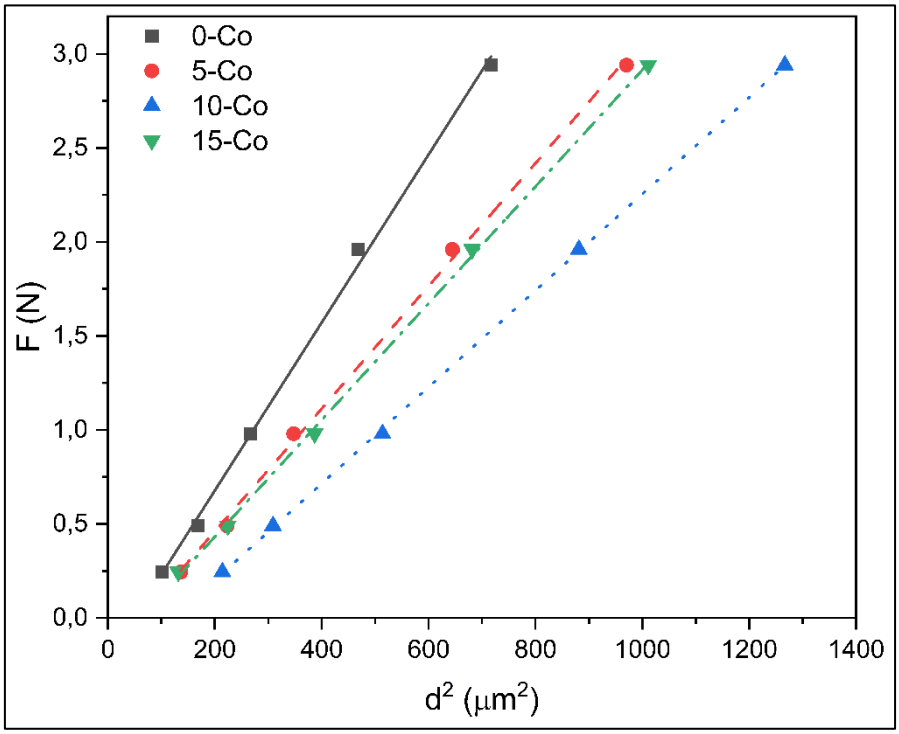

Figure 4. F-d^2 graph of the samples produced.

3.3. Elastic plastic deformation

The model can be used to determine whether a material exhibits ISE or RISE behavior based on elastic recovery mechanism known as the elastic plastic deformation (EPD). This model is particularly utilitarian if the material exhibits a significant amount of inelastic deformation. The reason that, this model includes a utilitarian term in the formula that accounts for plastic deformation, thus emphasizing the role of plastic deformation.

$$F = A_{EPD}(d_e + d)^2 \tag{4}$$

Here is the formula to evaluate the expression of impression diagonal length within the plastic deformation (Rahal et al., 2017). In the formula d measured experimentally, de and A_{EPD} calculated from the $F^{1/2}$-d graph (Figure 5). All the materials studied showed a characteristic RISE behavior when subjected to applied test loads, as indicated by the minus de calculated for each sample produced. This is the result of the materials exhibiting the typical RISE nature when subjected to different applied loads. In addition, negative de values confirms that no elastic deformation occurs in the system.

The true microhardness value for EPD model calculates via following formula;

$$H_{EPD} = 1854.4\, A_{EPD} \tag{5}$$

Table 4 includes the calculated true microhardness values and EPD model is not a sufficient method for calculating true microhardness for samples produced.

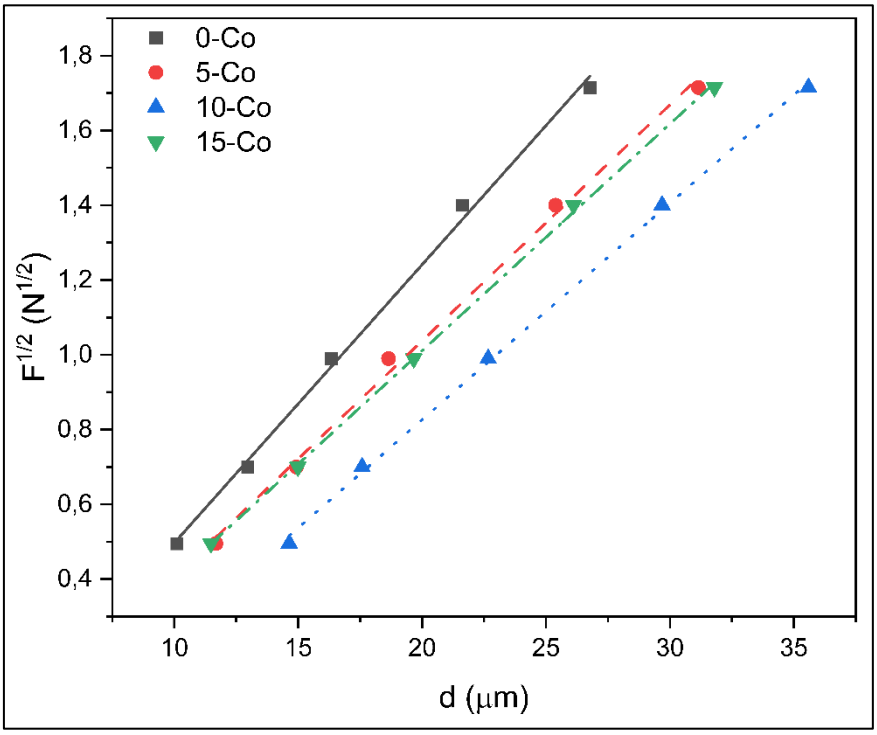

Figure 5. $F^{1/2}$-d graph of the samples produced.

Table 4. Load independent and load dependent microhardness values.

Sample	H_{HK} (GPa)	H_{EPD} (GPa)	H_{PSR} (GPa)	H_{IIC}(GPa)	H_V (GPa)
0-Co	8.289	10.276	9.828	7.576	6.8 - 7.607
5-Co	6.045	7.393	7.102	5.608	5.226 - 5.618
10-Co	4.766	6.219	5.804	4.075	3.535 - 4.304
15-Co	5.749	6.824	6.620	5.344	4.695 - 5.391

3.4. Proportional sample resistance

The proportional sample resistance (PSR) is a model that established on the energy dispersion caused by flaws, voids on the surfaces and cracks on visible parts of the material. It uses parameters (α and β) for describing the ISE/RISE nature of materials. The model is identified through the relationship between the true microhardness (load-independent) constant and surface energy (Saritekin & Üzümcü, 2022; Zalaoglu et al., 2020).

$$F = \alpha d + \beta d^2 \tag{6}$$

The graph (Figure 6) illustrates the linearly fitted F/d and d for PSR model. β, one of the parameters in PSR comes from the slope of the F/d vs d graph, is used for calculating the true microhardness (load-independent) value using the formula below;

$$H_{PSR} = 1854.4\,\beta \tag{7}$$

All the produced samples exhibit a RISE behavior, as indicated by the α parameter which is negative (Table 3). β decreases with increasing Co nanoparticle doping level, indicating that the local structural distortions between the grains and strength of the grain boundaries decreases (Erdem et al., 2021). Load-independent microhardness values have calculated via Equation 7 are higher than plateau region. So, among the theoretical models applied to Co nanoparticle-doped YBCO-358 ceramics, PSR model gives the worst theoretical results for load-independent microhardness values.

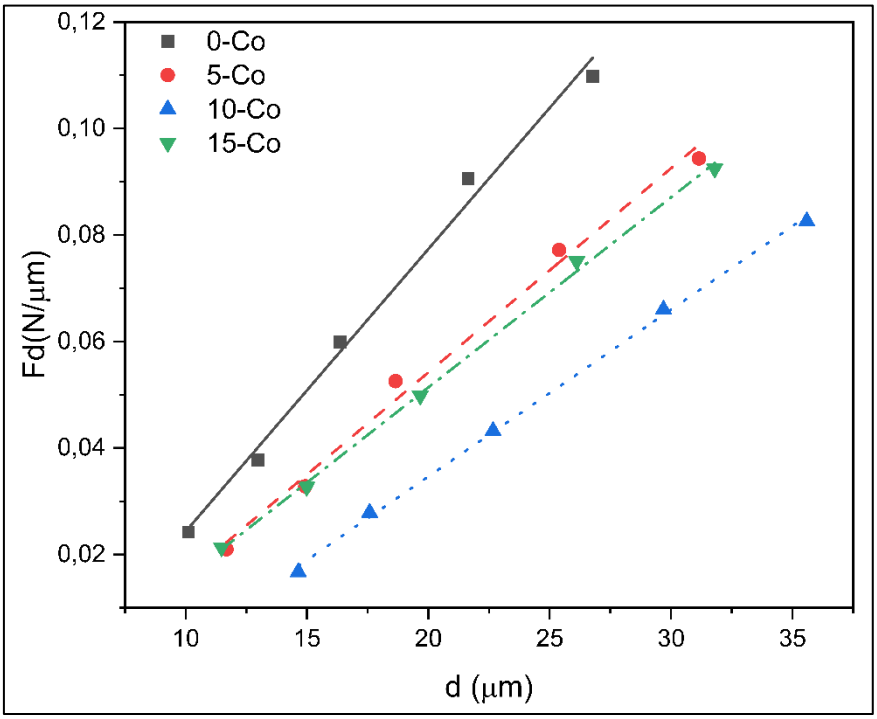

Figure 6. F/d-d graph of the samples produced.

3.5. Indentation-Induced cracking

The indentation-induced cracking (IIC) model is an effective way for examining the mechanical properties and behaviors of bulk polycrystalline YBCO ceramics. IIC model is useful for clarifying both ISE and RISE behavior that a material exhibits. The model considers four factors that affect the resistance to indentation diagonal size: crack mechanism, reversible and irreversible deformation, and indenter friction deformation. The formulation for the IIC model is presented below:

$$H_{IIC} = \lambda_1 K_1 (F/d^2) + K_2 \left(F^{5/3}/d^3\right) \tag{8}$$

in the equation, λ_1 is a constant that specific to the material being studied. K_1 offers the shape of the indentation tip, K_2 represents the test load that applied to the surface of the substance. If the material being studied exhibits perfect brittle behavior the value of λ_1 will be 0 (Farhat et al., 2019; Safran et al., 2015). The resulting equation becomes K_2 ($F^{5/3}/d^3$), and the final of this modified equation is;

$$H_{IIC} = K \left(\frac{F^{5/3}}{d^3}\right)^m \tag{9}$$

K and m values in the equation 9 are from the graph of $\ln(F^{5/3}/d^3)$ versus $\ln(H_V)$ (Figure 7). Calculated results for m, K and the true microhardness (H_{IIC}) are in the Table 3 and Table 4.

The IIC model showed the best fit among all models examined in this study. The m in the IIC, describes the RISE and ISE behavior. In the situations of "m>0.6" and "m<0.6"; ISE and RISE behavior attributes to material, respectively. In this study calculated m values indicates that Co nanoparticle doped YBCO-358 ceramic samples show RISE behavior (Terzioglu et al., 2019). The reduce in the load-independent microhardness value values of the doped YBCO-358 samples with increasing Co nanoparticle content, like the experimentally measured hardness values are visible in the Table 4. The load-independent microhardness value of the 0-Co calculated using the indentation-induced cracking model (H_{IIC} = 7.5758 GPa) falls within the saturation region that obtained by the experimentally handled microhardness values (6.8 - 7.607 GPa), which is eligible for the samples produced.

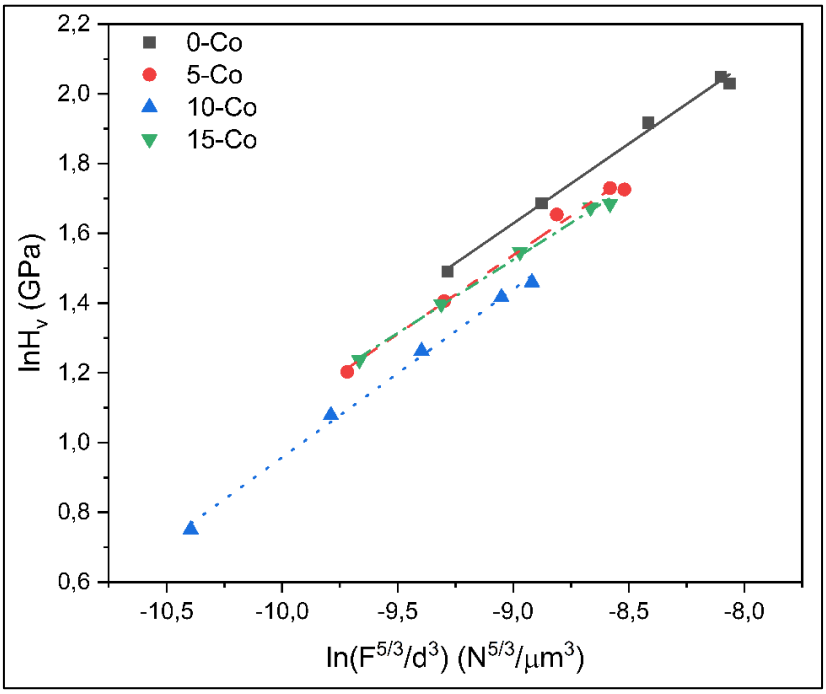

Figure 7. $\ln(F^{5/3}/d^3)$-$\ln H_V$ graph of the samples produced.

4. Conclusion

The microhardness properties and related theoretical approximations of YBCO-358 ceramics with Co nanoparticle doped at different rates were examined. This study scrutinizes the effects of Co nanoparticle doping on the hardness properties and the computed load-independent (true) hardness values of the YBCO-358 samples produced. It was observed that elastic modulus (E) and brittleness index (K_{IC}) values tended to reduce by the enlarging of doping ratio for produced samples. By increasing the doping Co concentration to the matrix microhardness values of the samples have been reduced. The reduction can be attributed to possible benefits to applications of the superconducting samples. When the Vickers microhardness properties are examined, the load-independent hardness values have been investigated by applying the Meyer's law, Hays-Kendall, elastic/plastic deformation, proportional sample resistance and the indentation-induced cracking methods, respectively, to the samples exhibiting RISE behavior. Using the mentioned models, the mechanical behavior of Co nanoparticle doped YBCO-358 samples has been examined and it has seen that the obtained parameters support the RISE behavior. The IIC model is successful in evaluating the true-microhardness values because it not only accurately describes the material's behavior but also provides the true-microhardness (load-independent) values in the plateau region that are experimentally obtained via microhardness measurement.

Acknowledgement

The Vicker's microhardness analyzes were carried out at Kastamonu University Central Research Laboratory.

Author contribution

The entire article was written by the primary author.

Declaration of ethical code

The author of this article declares that the materials and methods used in this study do not require ethics committee approval and/or legal-specific permission.

Conflicts of interest

The author declares that there is no conflict of interest.

References

Anas, M., Ebrahim, S., Eldeen, I. G., Awad, R. & Abou-Aly, A. I. (2017). Effect of single and multi-wall carbon nanotubes on the mechanical properties of Gd-123 superconducting phase. *Chemical Physics Letters*, 686, 34–43. https://doi.org/10.1016/j.cplett.2017.08.016

Asikuzun, E. & Ozturk, O. (2018). Theoretical and experimental approaches to measuring mechanical properties of Zn1−xCoxO binary tetrahedral bulk semiconductors. *Journal of Materials Science: Materials in Electronics*, 29(10), 7971–7978. https://doi.org/10.1007/s10854-018-8800-2

Asikuzun, E., Ozturk, O., Aydemir, G. A. & Tasci, A. T. (2019). The Effect of Zinc on the Structural, Electrical, and Mechanical Properties of YBCO-123 Superconducting Nanoparticles Prepared by an Acetate-Based Sol-Gel Process. *Journal of Superconductivity and Novel Magnetism*, 32(11), 3415–3423. https://doi.org/10.1007/s10948-019-5127-z

Awad, R., Abou Aly, A. I., Kamal, M. & Anas, M. (2011). Mechanical Properties of (Cu0.5Tl0.5)-1223 Substituted by Pr. *Journal of Superconductivity and Novel Magnetism*, 24(6), 1947–1956. https://doi.org/10.1007/s10948-011-1150-4

Badreddine, K., Srour, A., Awad, R. & Abou-Aly, A. I. (2020). The investigation of mechanical and dielectric properties of Samarium doped ZnO nanoparticles. *Materials Research Express*, 7(2), 025016. https://doi.org/10.1088/2053-1591/ab7064

Dey, A. & Mukhopadhyay, A. K. (2014). *Nanoindentation of Brittle Solids*. CRC Press. https://doi.org/10.1201/b17110

Dogruer, M., Gorur, O., Karaboga, F., Yildirim, G. & Terzioglu, C. (2013). Zr diffusion coefficient and activation energy calculations based on EDXRF measurement and evaluation of mechanical characteristics of YBa2Cu3O7−x bulk superconducting ceramics diffused with Zr nanoparticles. *Powder Technology*, 246, 553–560. https://doi.org/10.1016/j.powtec.2013.06.018

Erdem, U., Akkurt, B., Ulgen, A. T., Zalaoglu, Y., Turgay, T. & Yildirim, G. (2021). Effect of annealing ambient conditions on crack formation mechanisms of bulk Bi-2212 ceramic systems. *Journal of Asian Ceramic Societies*, 9(3), 1214–1227. https://doi.org/10.1080/21870764.2021.1952746

Farhat, S., Rekaby, M. & Awad, R. (2019). Vickers microhardness and indentation creep studies for erbium-doped ZnO nanoparticles. SN Applied Sciences, 1(6), 546. https://doi.org/10.1007/s42452-019-0559-4

Hays, C. & Kendall, E. G. (1973). An analysis of Knoop microhardness. *Metallography*, 6(4), 275–282. https://doi.org/10.1016/0026-0800(73)90053-0

Imran, M., Khan, M. Z., Waqee-Ur-Rehman, M., Ullah, A., Ahmed, S., Nadeem, K. & Mumtaz, M. (2020). Role of Co3O4 Nanoparticles Addition in Infield Superconducting Properties of CuTl-1223 Phase. *Journal of Low Temperature Physics*, 200(3–4), 152–163. https://doi.org/10.1007/s10909-020-02488-1

Kölemen, U., Uzun, O., Yılmazlar, M., Güçlü, N. & Yanmaz, E. (2006). Hardness and microstructural analysis of Bi1.6Pb0.4Sr2Ca2−xSmxCu3Oy polycrystalline superconductors. *Journal of Alloys and Compounds*, 415(1–2), 300–306. https://doi.org/10.1016/j.jallcom.2005.09.023

Koralay, H., Arslan, A., Cavdar, S., Ozturk, O., Asikuzun, E., Gunen, A. & Tasci, A. T. (2013). Structural and mechanical characterization of Bi1.75Pb0.25Sr2Ca2Cu3−xSnxO10+y superconductor ceramics using Vickers microhardness test. *Journal of Materials Science: Materials in Electronics*, 24(11), 4270–4278. https://doi.org/10.1007/s10854-013-1396-7

Mohammed, N. H., Abou-Aly, A. I., Ibrahim, I. H., Awad, R. & Rekaby, M. (2011). Effect of Nano-Oxides Addition on the Mechanical Properties of (Cu0.5Tl0.5)-1223 Phase. *Journal of Superconductivity and Novel Magnetism*, 24(5), 1463–1472. https://doi.org/10.1007/s10948-010-0853-2

Ozturk, O., Asikuzun, E., Tasci, A. T., Gokcen, T., Ada, H., Koralay, H. & Cavdar, S. (2018). Comparison of Vickers microhardness of undoped and Ru doped BSCCO glass ceramic materials. *Journal of Materials Science: Materials in Electronics*, 29, 3957–3966. https://doi.org/10.1007/s10854-017-8336-x

Rahal, H. T., Awad, R., Gaber, A. M. A. & Roumie, M. (2017). Superconducting and Mechanical Properties of the Bulk (SnO2) x (Bi1.6Pb0.4)Sr2Ca2Cu3O10−δ Prepared at Different Sintering Times. *Journal of Superconductivity and Novel Magnetism*, 30(7), 1971–1980. https://doi.org/10.1007/s10948-016-3654-4

Rekaby, M., Mohammed, N. H., Ahmed, M. & Abou-Aly, A. I. (2022). Synthesis, microstructure and indentation Vickers hardness for (Y3Fe5O12)x/Cu0.5Tl0.5Ba2Ca2Cu3O10-δ composites. *Applied Physics A*, 128(4), 261. https://doi.org/10.1007/s00339-022-05394-3

Safran, S., Kılıç, A., Kılıçarslan, E., Ozturk, H., Alp, M., Asikuzun, E. & Ozturk, O. (2015). Mechanical, microstructural and magnetic properties of the bulk BSCCO superconductor prepared by two different methods. *Journal of Materials Science: Materials in Electronics*, 26(4), 2622–2628. https://doi.org/10.1007/s10854-015-2733-9

Sahoo, B., Mohapatra, S. R., Singh, A. K., Samal, D. & Behera, D. (2019). Effects of CNTs blending on the superconducting parameters of YBCO superconductor. *Ceramics International*, 45(6), 7709–7716. https://doi.org/10.1016/j.ceramint.2019.01.072

Sahoo, B., Routray, K. L., Mirdha, G. C., Karmakar, S., Singh, A. K., Samal, D. & Behera, D. (2019). Investigation of microhardness and superconducting parameters of CNTs blended YBCO superconductor. *Ceramics International*, 45(17), 22055–22066. https://doi.org/10.1016/j.ceramint.2019.07.222

Sangwal, K. (2000). On the reverse indentation size effect and microhardness measurement of solids. *Materials Chemistry and Physics*, 63(2), 145–152. https://doi.org/10.1016/S0254-0584(99)00216-3

Saritekin, N. K. & Üzümcü, A. T. (2022). Improving Superconductivity, Microstructure, and Mechanical Properties by Substituting Different Ionic Pb Elements to Bi and Ca Elements in Bi-2223 Superconductors. *Journal of Superconductivity and Novel Magnetism*, 35(9), 2259–2273. https://doi.org/10.1007/s10948-022-06209-5

Sarıtekin, N. K., Zalaoglu, Y., Yildirim, G., Doğruer, M., Terzioglu, C., Varilci, A. & Gorur, O. (2014). Determination of solid solubility level of Ho nanoparticles in Y-123 superconducting matrix and strong Cu1 site preference of nanoparticles. *Journal of Alloys and Compounds*, 610, 361–371. https://doi.org/10.1016/j.jallcom.2014.04.037

Sedky, A., Salah, A. & Abou-Aly, A. (2020). Normal and Superconducting Properties of Bi1.7Pb0.30Sr2Ca1−xLaxCu2Oy Superconductor with $0.00 \leq x \leq 0.30$. *Journal of Superconductivity and Novel Magnetism*, 33(11), 3349–3359. https://doi.org/10.1007/s10948-020-05587-y

Senol, S. D., Terzioglu, R. & Ozturk, O. (2019). The influence of boron doping on the structural and mechanical characterization of ZnO. *Journal of Alloys and Compounds*, 797, 717–726. https://doi.org/10.1016/j.jallcom.2019.05.140

Soykan, U., Valiyeva, F. & Yildirim, G. (2020). Examination of vanadium effect on general mechanical characteristics of bi-2223 materials via semi-empiric models. *Eskişehir Technical University Journal of Science and Technology A - Applied Sciences and Engineering*, 21, 91–100. https://doi.org/10.18038/estubtda.818446

Terzioglu, R., Altintas, S. P., Varilci, A. & Terzioğlu, C. (2019). Modeling of Micro-Hardness in the Au-Doped YBCO Bulk Superconductors. *Journal of Superconductivity and Novel Magnetism*, 32(11), 3377–3383. https://doi.org/10.1007/s10948-019-5117-1

Yao, C. & Ma, Y. (2021). Superconducting materials: Challenges and opportunities for large-scale applications. *IScience*, 24(6), 102541. https://doi.org/10.1016/j.isci.2021.102541

Zalaoglu, Y., Turgay, T., Ulgen, A. T., Erdem, U., Turkoz, M. B. & Yildirim, G. (2020). A novel research on the subject of the load-independent microhardness performances of Sr/Ti partial displacement in Bi-2212 ceramics. *Journal of Materials Science: Materials in Electronics*, 31(24), 22239–22251. https://doi.org/10.1007/s10854-020-04724-6